Deformation mechanism of nylon 6 gel and melt films estimated in terms of orientation distribution function of crystallites

Masaru Matsuo*, Reiko Sato, Naoko Yanagida and Yoshimi Shimizu
Department of Clothing Science, Faculty of Home Economics, Nara Women's University, Nara 630, Japan
(Received 4 December 1990; revised 12 March 1991; accepted 22 May 1991)

Nylon 6 films were prepared by gelation/crystallization from solutions. The solvents used were a formic acid–chloroform mixture, trifluoroethanol and benzyl alcohol. Maximum values for Young's modulus and the orientational degree of the b-axes (the crystal fibre axes), were obtained for the drawn films prepared from formic acid–chloroform solution. These values, however, were lower than those of melt films. To study the reason for this, the deformation mechanism of gel films prepared from the formic acid–chloroform cosolvent was investigated and compared with the deformation mechanism of melt film using the orientation distribution function of crystallites. The distribution functions of both films exhibited similar profiles, indicating the preferential orientation of the b-axis with respect to the stretching direction by the rotation of crystallites around the c-axis, leading to taut tie molecules. This mechanism was found to be quite different from the molecular orientation of ultradrawn polyethylene gel films associated with significant crystal transformation from a folded to a fibrous type.

(Keywords: nylon 6 film; gelation/crystallization; Young's modulus; orientation distribution function of crystallites; rotation of crystallites)

INTRODUCTION

Since 1974, the preparation of polymeric fibres and films with high modulus and high strength has been extensively investigated on the basis of the surface growth[1,2] and gel deformation method[3–6] and results of interest have been obtained for polyethylene. These investigations have made clear that an extremely high orientation of crystallites due to the significant crystal transformation from a folded to a fibrous type provides high modulus and high strength films and/or fibres and this orientational behaviour of crystallites is quite different from that of melt films associated with the rotation of crystallites leading to taut tie molecules[7].

Unfortunately, the application range of polyethylene is limited by the flexibility of the individual chains and low melting point. Therefore it is important to achieve ultradrawing of other crystalline polymers such as polyester and polyamides with a melting point higher than 200°C and with high molecular rigidity. Nylon 6 fibres are widely used, e.g. as tyre yarns, and extensive work has been done to investigate their morphological and mechanical aspects[8–16]. Super-high speed melt spinning[16] has been proposed as a method to produce high strength and high modulus fibres of nylon 6 on a commercial basis. According to Shimizu *et al.*[16] the orientational degree of molecular chains became larger as the velocity of the spinning increased. Their work, however, showed that beyond a velocity of 6000 m min^{-1}, non-uniform structures exist whose degree of molecular orientation, crystallinity and birefringence at the outer part of fibres are higher than those at the core; such a tendency becomes considerable with increasing velocity. Shimizu *et al.*[16] pointed out that such a radial variation becomes an obstacle to improving the mechanical properties of fibres. Nylon 6, however, is among the most difficult materials to elongate to a high draw ratio and to achieve a Young's modulus sufficiently high for commercial thermoplastics. The difficulty of ultradrawing nylon 6 is largely due to the presence of intermolecular hydrogen bonding between adjacent amide groups. They act as quash-crosslinks, inhibiting the sliding of chains along the hydrogen bond plane during drawing. In order to remove this defect, gel spinning has been developed for the production of nylon 6 instead of melt spinning.

Chauh and Porter[17] attempted to prepare a gel by dissolving nylon 6 in benzyl alcohol at 165°C and cooling down to room temperature. The resulting partially dried gel film was drawn by co-extrusion with poly(oxymethylene) as the outer billet at 150°C in an Instron rheometer up to a maximum draw ratio, λ, of 5.7. The Young's modulus reached 5.7 GPa for the specimens at draw ratios >3–7.

Gogolewski and Pennings[18] produced nylon 6 filaments by dry-spinning of solutions in cosolvent mixtures of formic acid–chloroform followed by hot-drawing at 200–240°C. The Young's modulus and tensile strength of the resultant nylon 6 fibres were strongly affected by the draw ratio, molecular weight and type of spinning solution. The best values of Young's modulus and tensile strength reached 19 GPa and 1 GPa, respectively.

In a previous paper[19], on the basis of the concept of Gogolewski and Pennings[18], the deformation mechanism of nylon 6 was studied using films prepared by gelation/

* To whom correspondence should be addressed

0032-3861/92/081640-09
© 1992 Butterworth-Heinemann Ltd.

crystallization from solutions with cosolvent mixtures of formic acid–chloroform in comparison with the deformation of a melt film. In preparing gel films, the formic acid–chloroform (F/C) compositions chosen were 100/0, 75/25 and 50/50. The morphology and mechanical properties of the resultant gel films were almost independent of the F/C composition. The Young's modulus and tensile strength of all the films were less than 4 and 0.2 GPa, respectively, since the maximum draw ratio was about 4. To study the origin of the poor drawability, the orientational behaviour of crystallites is discussed in this paper in terms of the orientation distribution function of crystallites proposed by Roe and Krigbaum[20,21]. Gel and melt films are used to investigate whether the deformation mechanism of nylon 6 gel and melt films are essentially the same. Furthermore, a possible way to improve drawability is studied using gel films prepared from trifluoroethanol[22,23] and benzyl alcohol[17], which have been reported as solvents of nylon 6.

EXPERIMENTAL

Nylon 6 with three values of weight average molecular weight, $\bar{M}_w = 6.3 \times 10^4$, 8.4×10^4 and 4.5×10^4, were used as test specimens. To obtain the $\bar{M}_w$ values, the viscosity average molecular weight ($\bar{M}_v$) was measured in m-cresol at 25°C and $\bar{M}_w$ was calculated according to the relationship between $\bar{M}_w$ and $\bar{M}_v$ as reported by Gogolewski and Pennings[18]. The solvents formic acid–chloroform, trifluoroethanol and benzyl alcohol were used to form gels by crystallization from solution.

Formic acid–chloroform mixture

The homogenized solution at a suitable concentration was poured onto a glass plate which was dipped into a water bath at 25–30°C to promote coagulation. The fresh gel films thus obtained were leached in running water for 1 day and dried under ambient conditions.

Trifluoroethanol

The homogenized solution was prepared at room temperature and was poured into an aluminium tray. The solvent was allowed to evaporate from the gels under ambient conditions.

Benzyl alcohol

The solutions were stabilized with 0.1% w/w antioxidant, 3-methyl-6-tert-butylphenol. Solutions were prepared by heating the well-blended polymer/solvent mixture at 140°C for 1 h under nitrogen. The homogenized solution was poured into an aluminium tray surrounded by ice water to form a gel. The solvent was allowed to evaporate from the gels under ambient conditions for 30 days.

All the specimens were vacuum-dried for 3 days prior to measurements in order to remove residual traces of solvent.

The gel films prepared from formic acid–chloroform mixture were stretched in a hot oven at 205°C under nitrogen. Gel films prepared from trifluoroethanol and benzyl alcohol were stretched in a silicon oil bath in the temperature range 215–220°C because of the difficulty of drawing in a hot oven at any temperature.

Densities of the specimens were measured by a pycnometer in carbon tetrachloride–toluene medium. Prior to measuring the density, the films were cut into fragments which were immersed in an excess of ethanol for 2 h in an ultrasonic washing instrument and subsequently vacuum-dried for 3 days.

The melting point was estimated in terms of melting endotherm of differential scanning calorimetry (d.s.c.) curves. Specimens weighing 5 mg were placed in a standard aluminium sample pan. Samples were heated at a constant rate of 10°C min^{-1} under nitrogen flow.

The X-ray measurements were carried out with a 12 kW rotating-anode X-ray generator (Rigaku RDA-rA) operated at 200 mA and 40 kV. Small angle X-ray scattering (SAXS) patterns were obtained by point focusing with a three-pin hole collimator system. The X-ray exposure time was 50 h. SAXS intensity distribution in the meridional direction was detected with a position-sensitive proportional counter (PSPC). The corrected intensity was obtained by subtracting the contribution of the background (corresponding to air scattering) from the total intensity. The counting interval exposure time was 4×10^5 s for both total and air scatterings.

The orientation distribution function of crystallites can be calculated on the basis of the orientation distribution functions of the reciprocal lattice vectors measured by X-ray diffraction, according to the method proposed by Roe and Krigbaum[20,21]. Measurements of the X-ray diffraction intensity distribution were performed using a horizontal scanning type goniometer, operating at a fixed time-step scan of 0.1°/20 s over a range of twice the Bragg angle, $2\theta_B$, from 13 to 54° and from 74.5 to 81° by rotating about the film normal direction at 2–5° intervals from 0 to 90°.

The intensity distribution was measured as a function of $2\theta_B$ at a given rotational angle, θ_j, and corrections were made for air scattering, background noise, polarization, absorption, incoherent scattering and amorphous contribution. The intensity curve thus obtained was assumed to be due to the contribution of the intensity from the crystalline phase. The intensity curve $I_{cry}(2\theta_B)$ was separated into the contribution from the individual crystal planes, assuming that each peak had a symmetric form given by a Lorentzian function of $2\theta_B$ in equation (1), where I_j^0 is the maximum intensity of the jth peak:

$$I_{cry}(2\theta_B) = \sum_j \frac{I_j^0}{1 + (2\theta_0^j - 2\theta_B)^2/(\beta_j)^2} \qquad (1)$$

Here β_j is the half-width of the jth peak at half the peak intensity and θ_0^j is the Bragg angle at which the maximum intensity of the jth peak appears. Using the same process at a given angle θ_j in the range from 0 to 90°, the intensity distribution $I_j(\theta_j)$ can be determined for the respective jth crystal plane, and the orientation distribution function of the jth reciprocal lattice vector may be given by:

$$2\pi q_j(\cos\theta_j) = \frac{I_j(\theta_j)}{\int_0^{\pi/2} I_j(\theta_j) \sin\theta_j \, d\theta_j} \qquad (2)$$

It should be noted that there are some crystal planes whose Bragg angle reflections are located very close to each other. In this case, the function $q_j(\cos\theta_j)$ for the respective crystal planes, except the (200) and (040) planes, cannot be represented because of the difficulty of peak separation. The composite function $q_j(\cos\theta_j)$

includes the contributions of several planes as follows:

$$2\pi q_j(\cos\theta_j) = 2\pi \sum_{i=1}^{N_j} C_{ji} q_{ji}(\cos\theta_j) \qquad (3)$$

The concept underlying equation (3) was first presented by Roe and Krigbaum[20,21]. N_j is the number of the jth superposed peaks and C_{ji} is the relative (normalized) weight for the vector r_{ji}. Before numerical calculation by computer initial values of C_{ji} are given by:

$$C_{ji} = \frac{F_{ji}}{\sum_{j=1}^{N_j} F_{ji}} \qquad (4)$$

where F_{ji} is the structure factor of the jth crystal plane.

The separation for the orientation distribution functions of the reciprocal lattice vectors of the (200) and (040) planes was done until the profile of the function of the (040) plane was almost equal to that of the (0140) plane. The detailed method is described elsewhere[19].

RESULTS AND DISCUSSION

Figure 1 shows wide-angle X-ray diffraction (WAXD) and SAXS patterns for the original film prepared from trifluoroethanol solution. The patterns were obtained with the incident beam directed to the film surface. The WAXD patterns show a uniplanar orientation of the (002) plane parallel to the film surface, indicating the preferential orientation of the b-axes (the crystal fibre axes). The SAXS patterns show the meridional scattering with a scattering maximum indicating that crystal lamellae are highly oriented with their large flat faces parallel to the film surface. The profiles of both patterns are essentially the same, independent of the concentration of solution. The WAXD and SAXS patterns together indicate that within the lamellar crystals constituting the gel, the b-axes are oriented parallel to the large flat faces. This is quite different from the morphological properties of polyethylene resembling mats of single crystals, the c-axis (the crystal fibre axis) being perpendicular to the large flat faces. Such profiles of the WAXD and SAXS patterns could be observed for the gels prepared from benzyl alcohol, while any preferential orientations of crystallites and crystal lamellae for the gels prepared from formic acid–chloroform cosolvent mixtures could not be confirmed by WAXD and SAXS patterns.

On the basis of the results in *Figure 1*, the long period was estimated from SAXS intensity distribution detected by PSPC. *Table 1* summarizes the result. At $\bar{M}_w = 4.5 \times 10^5$ and 8.4×10^4, the long period slightly decreases with increasing concentration and is almost independent of molecular weight. In contrast, the long period for the specimens prepared from benzyl alcohol solution with 6 g/100 ml is lower than that prepared from the trifluoroethanol solution with the same concentration.

Table 2 shows the melting point and crystallinity as a function of concentration and molecular weight for undrawn films prepared from trifluoroethanol solution and from cosolvent mixtures of formic acid–chloroform with different F/C compositions. To check the reappearance of the d.s.c. profile, measurements of each specimen were carried out three times. For the films prepared from trifluoroethanol solution, crystallinity increases with decreasing concentration. This supports the increase in long period with decreasing concentration. In contrast, the melting point is hardly affected by concentration. The

Table 1 Long period of undrawn nylon 6 gel films prepared from trifluoroethanol and benzyl alcohol solutions

Solvent	$\bar{M}_w$	Concentration (g/100 ml)	Long period (Å)
Trifluoroethanol	4.5×10^5	1.5	94
		3.0	90
		6.0	84
	8.4×10^4	3.0	91
		6.0	86
Benzyl alcohol	4.5×10^5	6.0	69

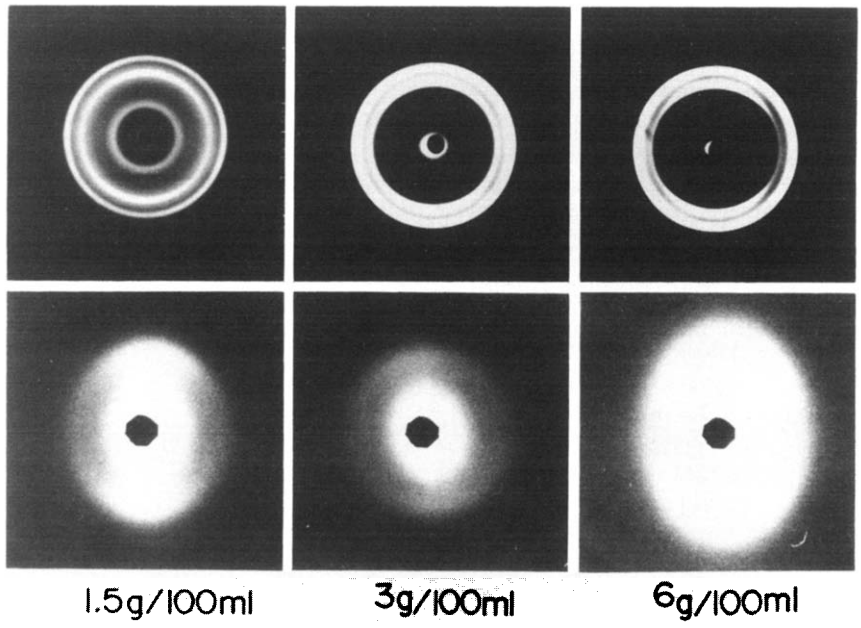

Figure 1 WAXD (top row) and SAXS (bottom row) patterns for undrawn gel films prepared from trifluoroethanol solutions with the indicated concentrations

Table 2 Melting point and crystallinity of undrawn gel films

Solvent	$\bar{M}_w$	Concentration (g/100 ml)	Crystallinity (%)	Melting point (°C)
Trifluoroethanol	4.5×10^5	1.5	–	223
		3	56.6	222
		6	43.5	223
		12	39.2	221
	8.4×10^4	3	53.7	219
		6	52.2	220
		12	46.6	219
Formic acid–chloroform				
F/C = 100/0	6.3×10^4	5	55.1	220
		10	52.0	220
		20	52.8	216
		30	48.2	218
F/C = 75/25	6.3×10^4	5	35.6	216
		10	32.4	217
		20	29.2	218
		30	30.0	220
F/C = 50/50	6.3×10^4	5	34.8	218
		10	34.0	217
		20	37.2	218
		30	40.4	218

melting point of the $\bar{M}_w = 4.5 \times 10^5$ specimen is slightly higher than that of the $\bar{M}_w = 8.4 \times 10^4$ specimen, indicating the larger size of crystallites. For the films prepared from the cosolution with different F/C compositions, the crystallinity of gel films prepared from only formic acid (100/0) solution decreases with increasing concentration, but even at 30 g/100 ml the value is higher than for films with other F/C compositions. The crystallinity of gel films with 75/25 composition shows a small decrease in the range 5–10 g/100 ml but is independent of concentration beyond 10 g/100 ml. The crystallinity of the gel with 50/50 composition increases at concentrations $\geqq$ 10 g/100 ml. Thus a clear relationship between crystallinity and concentration cannot be recognized. The melting point is almost independent of molecular weight, concentration and F/C composition.

Regarding drawing behaviour of films prepared from trifluoroethanol solution, observation revealed that at initial draw ratios <3, the deformation mechanism of the films is similar to that of polyethylene gel film consisting of two zones: unoriented and oriented. *Figure 2* shows WAXD patterns for drawn gel films prepared from trifluoroethanol with a concentration of 3 g/100 ml. As the draw ratio increases, the oriented regions elongate at the expense of the unoriented zone. The X-ray patterns indicate that in spite of the high draw ratio, the orientation of crystallites is not significant and the orientational degree is almost equal to that for films prepared from the formic acid–chloroform mixed solutions. This is attributed to the fact that elongation of the specimen is due not to molecular orientation but to slippage of polymer chains, similar to the drawing of amorphous poly(ethylene terephthalate) films in a hot water bath. Young's modulus and tensile strength are less than 3 GPa and 100 MPa, respectively. These values are less than those obtained for gel films prepared from formic acid–chloroform solution as well as those obtained from melt films. Incidentally, the orientational degree of crystallites within gel films prepared from benzyl alcohol was slightly lower than for films prepared from trifluoroethanol and consequently the Young's and tensile moduli were also slightly lower than the above values.

Table 3 shows the changes in crystallinity with draw ratio measured for the gel films prepared from trifluoroethanol and formic acid–chloroform solutions and for melt films. A drastic decrease in crystallinity of the gel films prepared from trifluoroethanol solution with concentration of 1.5 g/100 ml occurred at initial draw ratio up to $\lambda = 10$, indicating significant unfolding of the folded crystal; however, a further increase in crystallinity could

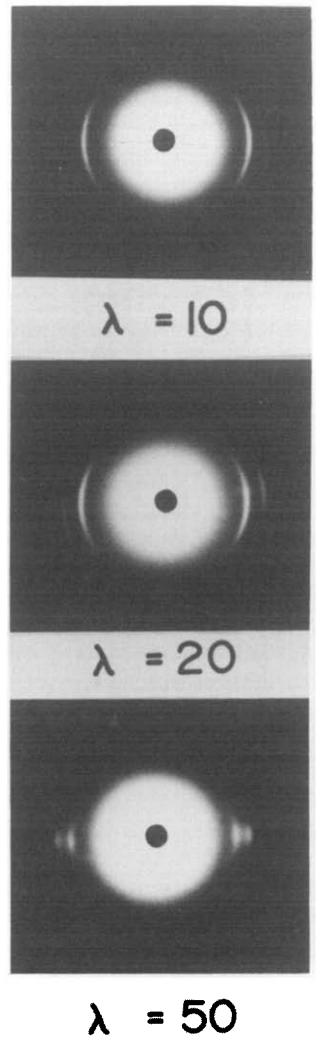

Figure 2 WAXD patterns for drawn gel film prepared from trifluoroethanol solution with a concentration of 3 g/100 ml

Table 3 Change in crystallinity with draw ratio measured for gel films and melt films. Gel films were prepared from trifluoroethanol solution and formic acid–chloroform solutions with 75/25 composition

	Crystallinity (%)		
	Gel films		
Draw ratio (λ)	Trifluoroethanol	Cosolvent (F/C = 75/25)	Melt films
1	56.6	30.0	25.1
2	–	41.4	36.8
4	–	47.7	41.9
5	–	–	46.6
10	21.9	–	–
20	27.6	–	–
50	30.2	–	–

not be achieved by further elongation. This indicates the difficulty in crystal transition from a disordered folded type to a fibrous type under elongation. Further elongation from $\lambda = 10$ to 20 is obviously attributed to molecular slippage rather than molecular orientation as discussed before. Accordingly, the crystallinity at the maximum draw ratio of 50 is much lower than for gel films prepared from formic acid–chloroform solution and melt film at $\lambda = 4$.

In order to study poor molecular orientation of nylon 6 gel films, the orientational behaviour was estimated in terms of the orientation distribution function of crystallites. The gel films prepared from formic acid–chloroform solution with 75/25 composition were used as test specimens, since the molecular orientation in an undeformed state is perfectly random without any uniplanar orientation of a particular crystal plane parallel to the film surface, and the Young's modulus is higher than for films prepared from trifluoroethanol, benzyl alcohol solutions and formic acid–chloroform solutions with 100/0 and 50/50 compositions[19]. Incidentally, it may be noted that the orientation distribution functions of crystallites within the films prepared from trifluoroethanol and benzyl alcohol solutions must be estimated as a biaxial orientational system. However, this is impossible due to an insufficient number of crystal planes to assure correct values of the orientation factor of the reciprocal lattice vector of each crystal plane.

On the basis of the geometrical arrangements by Roe and Krigbaum[20,21], we shall consider crystal structures of nylon 6 in which a Cartesian coordinate system $O\text{-}U_1U_2U_3$ is fixed in such a way that the U_1, U_2, and U_3 axes are parallel to the reciprocal lattice vector of the (200) plane, c-axis and b-axis, respectively, making the properties of this coordinate system orthorhombically symmetric. The orientation of a given vector r_j (reciprocal lattice vector of the jth crystal plane) is represented with respect to the polar and azimuthal angles Θ_j and Φ_j within the coordinate $O\text{-}U_1U_2U_3$. *Table 4* shows the results.

For a uniaxial system, the orientation distribution function $\omega(\cos\theta, \eta)$ of crystallites may be calculated from $2\pi q_j(\cos\theta_j)$ using a method proposed by Roe and Krigbaum[20,21]:

$$F_{l0}^j = \langle P_l(\cos\theta_j)\rangle = \int_0^{2\pi}\int_0^{\pi} q_j(\cos\theta_j)P_l(\cos\theta_j)\sin\theta_j\,d\theta_j\,d\phi_j \quad (5)$$

$$F_{l0}^j = F_{l00}\sum_i^{N_j} C_{ji}P_l(\cos\Theta_{ji}) + 2\sum_{n=2}^{l}\frac{(l-n)!}{(l+n)!}\left\{F_{l0n}\sum_i^{N_j} C_{ji}P_l^n(\cos\Theta_{ji})\cos n\Phi_{ji} + G_{l0n}\sum_{n=2}^{N_i} C_{ji}P_l^n(\cos\Theta_{ji})\sin n\Phi_{ji}\right\} \quad (6)$$

$$4\pi^2\omega(\cos\theta,\eta) = \frac{1}{2} + \sum_{l=2}^{\infty}\frac{(2l+1)}{2}\times\left\{F_{l00}P_l(\cos\theta) + 2\sum_{n=2}^{l}\frac{(l-n)!}{(l+n)!}\times\{F_{l0n}\cos n\eta + G_{l0n}\sin n\eta\}P_l^n(\cos\theta)\right\} \quad (7)$$

Table 4 Diffraction angle $2\theta_B$, and polar and azimuthal angles Θ_j and Φ_j in regard to the orientation of reciprocal lattice vector of the jth crystal plane within nylon 6 crystal (α type) unit

(hkl)	$2\theta_B$	Θ_j	Φ_j
(200)	20.11	0	0
(040)	20.61	0	0
(002)	24.05	90	−61.5
(202)	24.78	90	63.77
(160)	32.78	18.02	0
(001)	33.45	21.22	−61.5
($\bar{2}$02)	37.20	90	−37.12
(162)	38.58	35.68	87.75
(402)	38.68	90	35.55
($\bar{1}$71)	41.14	27.00	−37.12
(271)	41.48	27.87	35.55
($\bar{2}$71)	46.09	36.90	−24.17
(371)	46.62	37.70	23.44

Here l and n are even integers. $P_l^n(x)$ and $P(x)$ are the associated Legendre polynomials and Legendre polynomials, respectively. The coefficients F_{l0}^j, F_{l0n} and G_{l0n} may be represented by the coefficients α_{l0}^j, A_{l0n} and B_{l0n} given by Roe and Krigbaum[20]:

$$F_{l0}^j = \left\{\frac{2}{2l+1}\right\}^{1/2} 2\pi\alpha_{l0}^j \quad (8)$$

$$F_{l0n} = \left\{\frac{2}{2l+1}\frac{(l+n)!}{(l-n)!}\right\}^{1/2} 4\pi^2 A_{l0n} \quad (9)$$

$$G_{l0n} = \left\{\frac{2}{2l+1}\frac{(l+n)!}{(l-n)!}\right\}^{1/2} 4\pi^2 B_{l0n} \quad (10)$$

The coefficients F_{l0n} and G_{l0n} can be determined by solving the linear equations represented by equation (6), since there exist more equations than the number of unknowns, as was pointed out by Roe and Krigbaum[20,21].

The values of weighting factors ρ_j, required in the least-squares calculation, were assigned somewhat subjectively on the assumption that the X-ray diffraction intensity is dependent upon the structure factor of each crystal plane. Hence, in this calculation, the weighting factors ρ_j, as a first approximation, were assumed to be almost proportional to the structure factor and were subsequently modified to obtain the best fit between experimental and calculated results through numerical calculations by computer.

Following Roe and Krigbaum[20,21], the values of F_{l0n} and G_{l0n} were determined by the least-squares method. In doing so, the values of C_{ji} were determined by the simplex method which is a direct search method to obtain the object function on the basis of trial and error[23]. The initial values of C_{ji} used in the simplex method were defined by equation (4), based on the structure factors F_{ji}. The calculation was continued until the best fit was achieved within the capability of the simplex method. Using the final values of parameters, a mean-square error between the calculated F_{l0}^j and recalculated F_{l0}^j was obtained using:

$$R = \frac{\sum_j\sum_l \rho_j[(F_{l0}^j)_{cal} - (F_{l0}^j)_{recal}]^2}{\sum_j\sum_l[(F_{l0}^j)_{cal}]^2} \quad (11)$$

Figures 3 and *4* compare the observed orientation distribution functions $2\pi q_j(\cos\theta_j)$ with those recalculated for the respective crystal planes for the gel and melt films, respectively, at $\lambda = 2$. *Figures 5* and *6* compare the

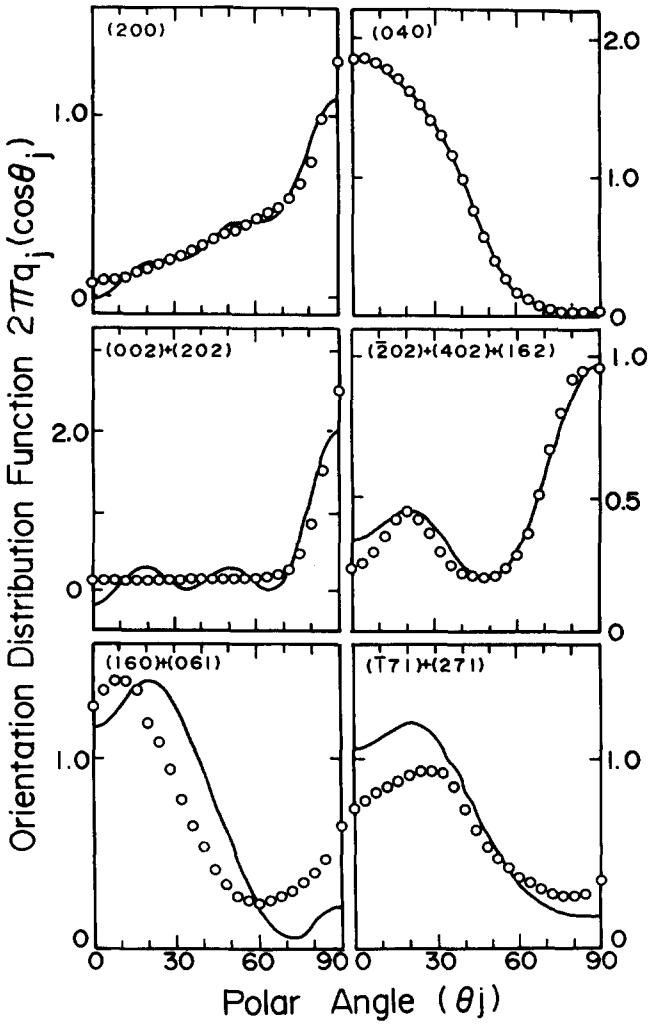

Figure 3 Orientation distribution functions $2\pi q_j(\cos\theta_j)$ of the reciprocal lattice vectors of the indicated crystal planes of nylon 6 gel film with $\lambda = 2$. ○, Values of $2\pi q_j(\cos\theta_j)$ obtained from experimental measurements; ——, $2\pi q_j(\cos\theta_j)$ calculated with 11 term series (l up to 10) with the use of recalculated F^j_{l0} values

observed orientation function $2\pi q_j(\cos\theta_j)$ with those recalculated for the respective crystal planes for the gel and melt films, respectively, at $\lambda = 4$. We calculated the best values of F_{l0n} and G_{l0n} from equation (6) to minimize the value of R in equation (11). After that, we recalculated F^j_{l0}, in turn, from the values of F_{l0n} and G_{l0n}, and further calculated $2\pi q_j(\cos\theta_j)$ from the recalculated F^j_{l0} value using the following equation:

$$2\pi q_j(\cos\theta_j) = \frac{1}{2}\sum_{l=2}^{\infty}\frac{(2l+1)}{2}F^j_{l0}P_l(\cos\theta_j) \quad (12)$$

Table 5 shows the values of ρ_j and C_{ji} for the (hkl) plane to obtain full curves in *Figures 3–6*. Values of R were calculated using the values of C_{ij} and ρ_j; for gel and melt films respectively, the values were 37.6% and 23.7% at $\lambda = 2$, and 46.8% and 44.4% at $\lambda = 4$.

Returning to *Figures 3–6*, it is evident that fairly good agreement between the observed and calculated distribution functions was obtained, even for the less accurately superposed crystal planes with lower weighting factors. The oscillations of the full curves are due to the procedure of expanding each sharp distribution function into an infinite series of spherical harmonics. This is an expected deficiency of this method. Actually, such oscillations could be observed for sharp distribution functions measured for ramie and mercerized ramie[24] but they have never been observed for more common, less sensitive distribution functions used to investigate the deformation mechanism of polyethylene spherulite[25].

Figure 7 shows the orientation distribution functions of crystallites $\omega(\cos\theta, \eta)$ calculated using equation (7) with the coefficients F_{l0n} and G_{l0n} determined from equation (6) with l limited to 10 or 12. As can be seen from the figures, several highly populated regions and negative regions exist, which complicate the detailed analysis of the deformation mechanism of nylon 6 films. Most of these regions must be artifacts of expansion of

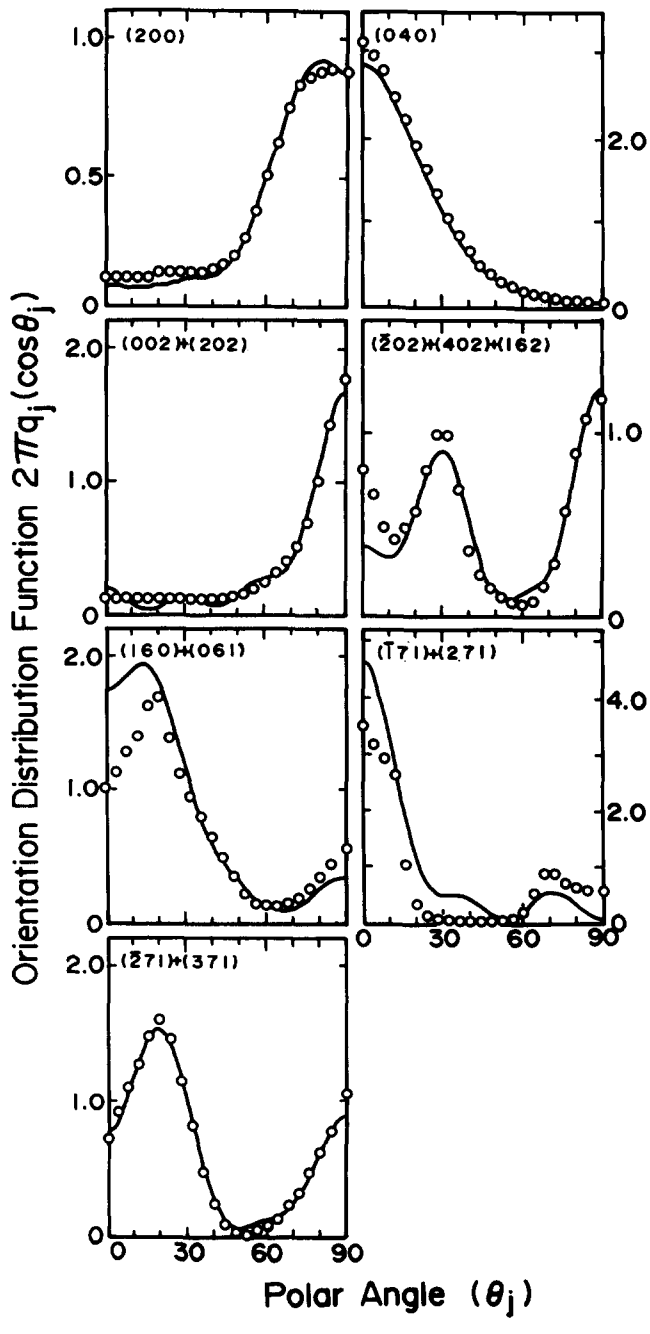

Figure 4 Orientation distribution functions $2\pi q_j(\cos\theta_j)$ of the reciprocal lattice vectors of the indicated crystal planes of nylon 6 melt film with $\lambda = 2$. ○, Values of $2\pi q_j(\cos\theta_j)$ obtained from experimental measurements; ——, $2\pi q_j(\cos\theta_j)$ calculated with 13 term series (l up to 12) with the use of recalculated F^j_{l0} values

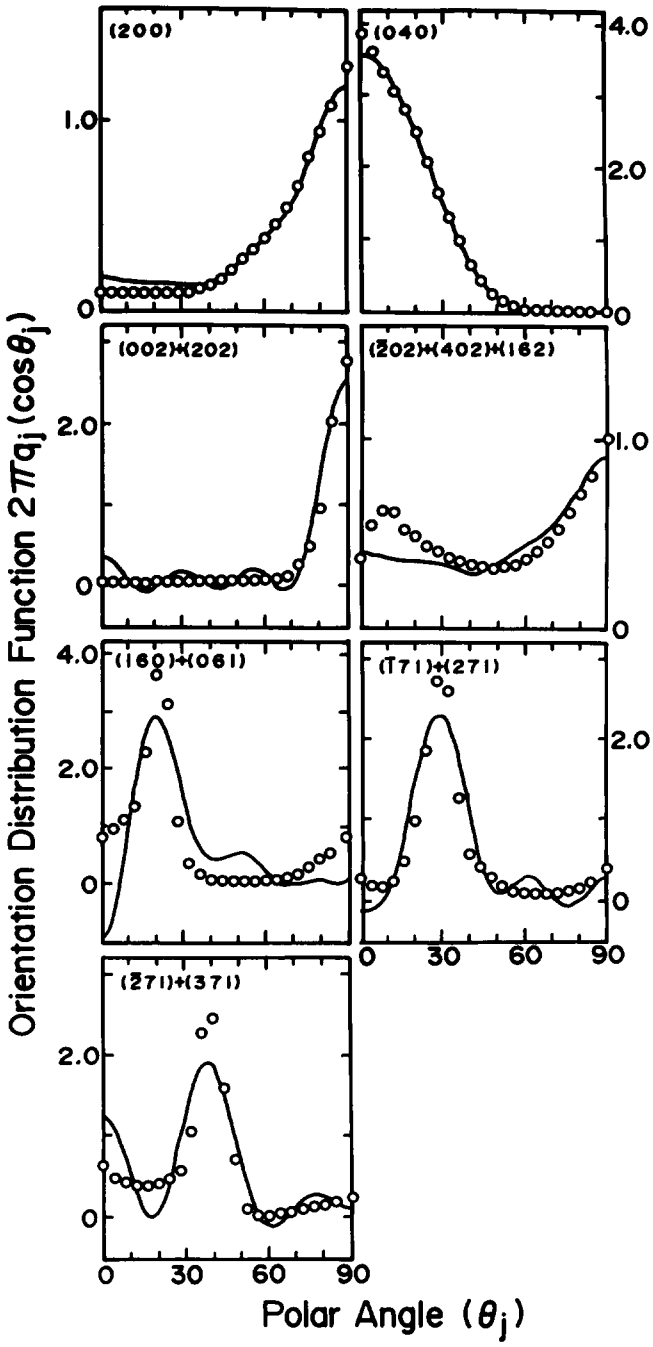

Figure 5 Orientation distribution functions $2\pi q_j(\cos\theta_j)$ of the reciprocal lattice vectors of the indicated crystal planes of nylon 6 gel film with $\lambda = 4$. ○, Values of $2\pi q_j(\cos\theta_j)$ obtained from experimental measurements; ——, $2\pi q_j(\cos\theta_j)$ calculated with 13 term series (l up to 12) with the use of recalculated F_{l0}^j values

the sharp experimental functions $2\pi q_j(\cos\theta_j)$ into infinite series of spherical harmonics. This tendency seems to be more pronounced as the polar angle θ becomes wider. Unfortunately, we could not demonstrate this, because when the sharp peaks at $\theta \geqq 60°$ were eliminated, the functions $2\pi q_j(\cos\theta_j)$ recalculated from $\omega(\cos\theta, \eta)$ (the value being zero at $\theta \geqq 60°$) were in poor agreement with the experimental results. The function of $\omega(\cos\theta, \eta)$ is symmetric at $\theta = 0°$ and thus

$$\omega(\cos\theta, \eta) = \omega(\cos\theta, \pi + \eta).$$

It is seen that in the range of η from 0 to 180°, $\omega(\cos\theta, \eta)$ shows considerable dependence on η, having highly populated regions at $\eta = 40$–$150°$ and $\eta = 140$–$160°$ for gel and melt films with $\lambda = 2$, and at $\eta = 40$–$50°$ and $\eta = 110$–$120°$ for gel and melt films with $\lambda = 4$. Interestingly, the maximum population of $\omega(\cos\theta, \eta)$ does not appear at $\theta = 0$. On average, however, the distribution function of the b-axis, corresponding to the reciprocal lattice vector of the (0 4 0) plane (and the (0 14 0) plane), has only a maximum peak at $\theta_j = 0$, which is indicative of the preferential orientation of the b-axes with respect to the stretching direction. Thus it appears that the profile of the orientation distribution function $\omega(\cos\theta, \eta)$ is not similar to that of the b-axis obtained by integration of $\omega(\cos\theta, \eta)$ with η in the range from 0 to 180°.

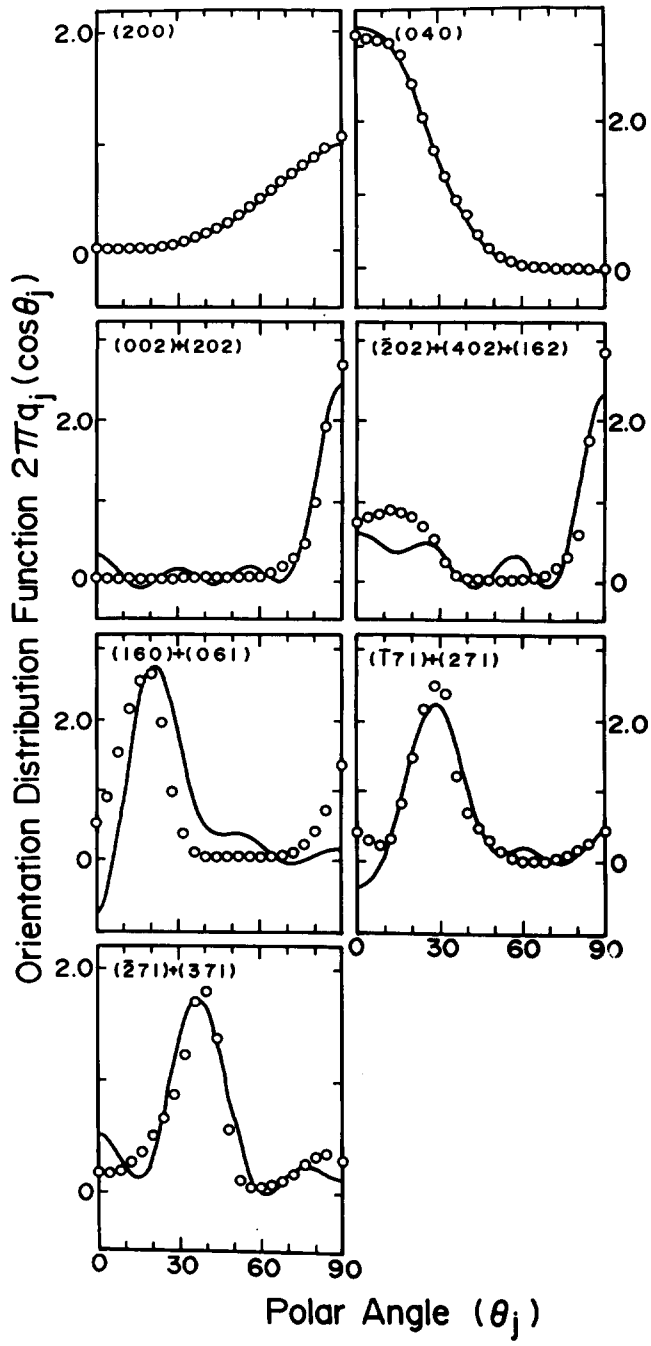

Figure 6 Orientation distribution functions $2\pi q_j(\cos\theta_j)$ of the reciprocal lattice vectors of the indicated crystal planes of nylon 6 melt film with $\lambda = 4$. ○, Values of $2\pi q_j(\cos\theta_j)$ obtained from experimental measurements; ——, $2\pi q_j(\cos\theta_j)$ calculated with 13 term series (l up to 12) with the use of recalculated F_{l0}^j values

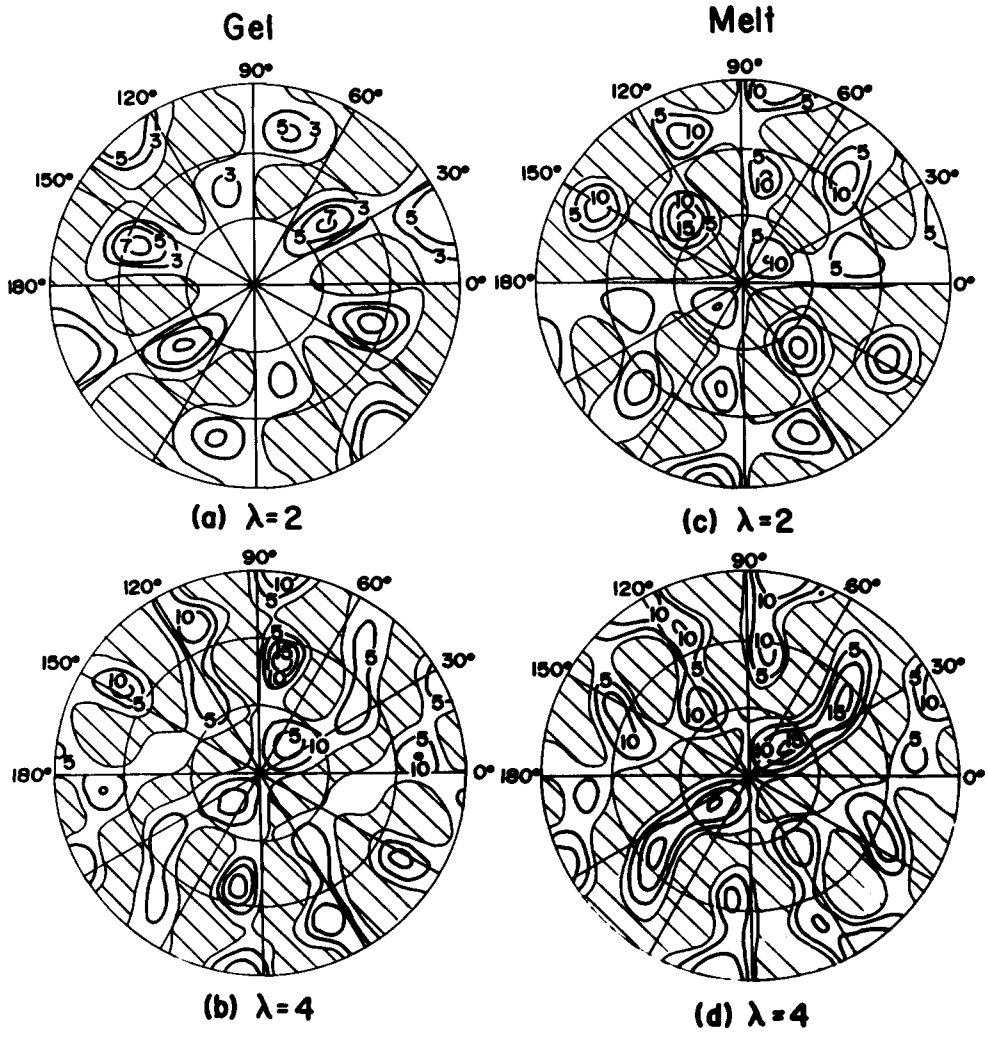

Figure 7 Orientation distribution functions of crystallites $\omega(\cos\theta, \eta)$ calculated with 13-term series of expansion from equations (5)–(7). (a) Gel film with $\lambda = 2$; (b) melt film with $\lambda = 2$; (c) gel film with $\lambda = 4$; (d) melt film with $\lambda = 4$

Table 5 Parameters for calculating the orientation distribution functions of the jth crystal plane of nylon 6 (α-type)

		C_{ji}			
(hkl)	ρ_j	Gel ($\lambda = 2$)	Melt ($\lambda = 2$)	Gel ($\lambda = 4$)	Melt ($\lambda = 4$)
(200)	1	1	1	1	1
(040)	1	1	1	1	1
(002)	1	0.999	0.999	0.999	0.999
(202)	1	0.001	0.001	0.001	0.001
(160)	0.034	0.501	0.999	0.501	0.502
(061)	0.034	0.499	0.001	0.499	0.498
($\bar{2}$02)	0.100	0.001	0.001	0.386	0.541
(162)	0.100	0.001	0.100	0.281	0.001
(402)	0.100	0.998	0.899	0.333	0.458
($\bar{1}$71)	0.132	0.999	0.999	0.999	0.999
(271)	0.132	0.001	0.001	0.001	0.001
($\bar{2}$71)	0.071		0.990	0.992	0.990
(371)	0.071		0.010	0.008	0.010

Here it should be noted that the profile of gel films prepared from formic acid–chloroform solution is similar to that of melt films at each draw ratio. This implies that the deformation mechanisms of the gel and melt films are almost the same and the preferential orientation of the b-axes is probably due to the rotation of crystallites leading to taut tie molecules which hamper ultradrawing.

Table 6 The second order orientation factors of the three principal crystallographic axes and amorphous chain segments

		Second order orientation factor			
Specimen	Draw ratio	a-axis	b-axis	c-axis	Amorphous chain segment
Gel film (75/25)	2	−0.192	0.527	−0.329	–
	4	−0.272	0.667	−0.393	–
Melt film	2	−0.252	0.528	−0.311	0.573
	4	−0.259	0.657	−0.395	0.743
	5	−0.340	0.716	−0.402	0.856

In order to support this concept, the orientation functions of amorphous chain segments are measured by subtraction of the amorphous contribution from the total birefringence[26]. Measurements of birefringence could not be made because of the difficulty in observing caused by whitening. *Table 6* summarizes the second order orientation factors of the amorphous chain segments in addition to those of the three principal crystallographic axes. These data have already appeared elsewhere[19]. The orientational degree of amorphous chain segments of the melt films is higher than that of the b-axes at $\lambda = 2$ and 4. This result supports the preferential orientation of the b-axes due to the rotation of crystallites leading to taut

tie molecules. To produce high modulus nylon 6 by gelation/crystallization from solution, it may be concluded that significant crystal transformation from a folded to a fibrous type is an important factor to ensure easy drawability, and that intermolecular hydrogen bonding must be eliminated by replacing the amide group with another non-polar group.

CONCLUSION

Nylon 6 films were prepared by gelation/crystallization from solutions. Formic acid–chloroform mixture, trifluoroethanol and benzyl alcohol were used as solvents. The WAXD and SAXS patterns indicated that original gel films from trifluoroethanol and benzyl alcohol solvents take a uniplanar orientation of the (200) plane and preferential orientation of the b-axes parallel to the film surface, and the crystal lamellae are highly oriented with their large flat faces parallel to the film surface. On the other hand, the original films prepared from formic acid–chloroform cosolvent mixture take a random orientation of crystallites and the SAXS patterns show no scattering maximum. Maximum values of Young's modulus and the orientational degree of the b-axes were obtained for the drawn gels prepared from the formic acid–chloroform mixture. The value of Young's modulus, however, was less than 4 GPa because of the poor draw ratio of less than 4. To study the poor drawability, the orientation of crystallites within the gel film prepared from formic acid–chloroform with 75/25 composition was studied in terms of the orientation distribution function of crystallites proposed by Roe and Krigbaum[20,21], and the results were compared with those of melt films. Both profiles at $\lambda = 2$ and 4 resembled each other indicating the preferential orientation of the b-axes not by significant crystal transformation from a folded to a fibrous type, but by rotation of crystallites around the c-axis leading to taut tie molecules. This behaviour is found to be different from the molecular orientation due to significant crystal transformation within polyethylene gel films ensuring ultradrawing.

REFERENCES

1 Smook, J., Torf, J. C., van Hulten, P. F. and Pennings, A. J. *Polym. Bull.* 1980, **2**, 293
2 Barham, P. J. and Keller, A. *J. Mater. Sci.* 1980, **15**, 2229
3 Smith, P., Lemstra, P. J., Kalb, B. and Pennings, A. J. *Polym. Bull.* 1979, **1**, 733
4 Smith, P. and Lemstra, P. J. *J. Mater. Sci.* 1980, **15**, 505
5 Smith, P., Lemstra, P. J., Pippers, J. P. L. and Kiel, A. M. *Colloid Polym. Sci.* 1981, **258**, 1070
6 Matsuo, M., Sawatari, C., Iida, M. and Yoneda, M. *Polym. J.* 1985, **17**, 1197
7 Nomura, S., Matsuo, M. and Kawai, H. *J. Polym. Sci.* 1972, **10**, 2489
8 Bunn, C. W. and Garner, E. V. *Proc. R. Soc. (London)* 1947, **A189**, 39
9 Takagai, J. and Hattori, H. J. *J. Appl. Polym. Sci.* 1965, **9**, 2167
10 Papir, Y. S., Kapur, S. and Rogers, C. E. *J. Polym. Sci., Part A-2* 1972, **10**, 1305
11 Coppaccio, G. and Ward, I. M. *Polym. Eng. Sci.* 1975, **15**, 219
12 Acierno, D., LaMantia, F. P., Polozotti, G., Alfonso, G. C. and Ciferri, A. *J. Polym. Sci., Polym. Lett. Edn.* 1977, **15**, 323
13 Richurdson, A. and Ward, I. M. *J. Polym. Sci., Polym. Phys. Edn.* 1981, **19**, 1549
14 Subramanian, D. R., Venkataraman, A. and Bkat, N. V. *J. Appl. Polym. Sci.* 1982, **27**, 4149
15 Leung, W. P., Ho, K. H. and Choy, C. L. *J. Polym. Sci., Polym. Phys. Edn.* 1984, **22**, 1173
16 Shimizu, J., Okui, N., Kikutani, T., Ono, A. and Takaku, A. *Sen-i-Gakkaishi* 1981, **37**, 143
17 Chauh, H. H. and Porter, R. S. *Polymer* 1986, **27**, 1022
18 Gogolewski, S. and Pennings, A. J. *Polymer* 1985, **26**, 1394
19 Matsuo, M. and Inaba, K. *Polym. J.* 1988, **20**, 965
20 Roe, R. J. and Krigbaum, W. R. *J. Chem. Phys.* 1964, **40**, 2608
21 Krigbaum, W. R. and Roe, R. J. *J. Chem. Phys.* 1964, **41**, 737
22 Rafler, G. and Reinisch, G. *Angew. Makromol. Chem.* 1971, **20**, 57
23 Spendly, W., Hext, G. and Himsworth, F. R. *Technometrics* 1962, **4**, 441
24 Matsuo, M., Sawatari, C., Iwai, Y. and Ozaki, F. *Macromolecules* 1990, **23**, 3266
25 Fujita, K., Suehiro, S., Nomura, S. and Kawai, H. *Polym. J.* 1982, **14**, 545
26 Stein, P. S. and Norris, F. H. *J. Polym. Sci.* 1956, **21**, 38